THE JOURNAL OF PHYSICAL CHEMISTRY A

Article

pubs.acs.org/JPCA

Stimulated Emission Enhancement Using Shaped Pulses

Arkaprabha Konar,[†] Vadim V. Lozovoy,[†] and Marcos Dantus*[,†,‡]

[†]Department of Chemistry and [‡]Department of Physics and Astronomy, Michigan State University, East Lansing, Michigan 48824, United States

Supporting Information

ABSTRACT: Controlling stimulated emission is of importance because it competes with absorption and fluorescence under intense laser excitation. We performed resonant nonlinear optical spectroscopy measurements using femtosecond pulses shaped by π- or $\pi/2$-step phase functions and carried out calculations based on density matrix representation to elucidate the experimental results. In addition, we compared enhancements obtained when using other pulse shaping functions (chirp, third-order dispersion, and a time-delayed probe). The light transmitted through the high optical density solution was dominated by an intense stimulated emission feature that was 14 times greater for shaped pulses than for transform limited pulses. Coherent enhancement depending on the frequency, temporal, and phase characteristics of the shaped pulse is responsible for the experimental observations.

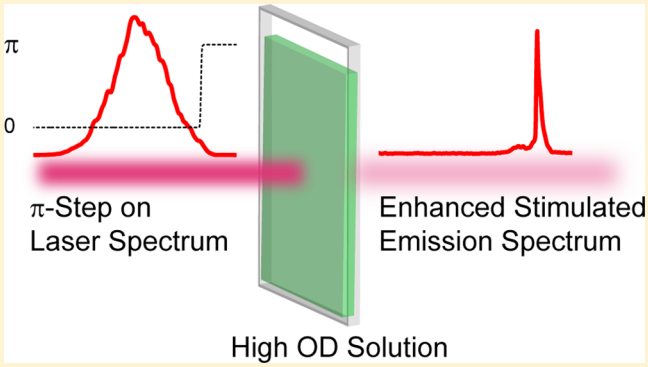

INTRODUCTION

The propagation of femtosecond pulses in optically dense media is affected by linear processes such as absorption and fluorescence and by nonlinear processes such as multiphoton excitation and stimulated emission. Stimulated emission as defined by Einstein is a coherent process independent of how population inversion was achieved. In the context of the present research, where a single femtosecond pulse is responsible for creating population inversion and stimulating emission, it is appropriate to consider stimulated emission to be the field emitted by the third- or higher-order polarization of the system and is therefore a subject of nonlinear optical spectroscopy.

Resonant ultrafast nonlinear optical spectroscopy has blossomed in the past three decades because nonlinear signals depend on frequency, time, and phase characteristics of the incident laser pulses and provide richer information than is available from linear spectroscopic methods.[1−5] Nonlinear four-wave mixing spectroscopies[6,7] measure the third-order polarization resulting from the coherent interaction of two or more laser pulses with the molecule, and the signal emitted by the sample is usually a coherent optical beam. Our research group has been developing nonlinear optical spectroscopic methods involving a single ultrafast shaped laser pulse in an effort to simplify experimental implementations through eliminating the need for multiple phase-related pulses.[8−10]

Early studies on fluorescence yield dependence on chirp found that positively chirped pulses led to greater fluorescence.[11] The findings were explained by invoking a wave packet following model whereby low frequency photons in the pulse deplete population in the excited state when negatively chirped pulses are used. Chirp was proposed as a means to control ground and excited state populations, and this control was later applied to photon echo studies.[12,13] Connection between depletion and enhanced stimulated emission confirmed control of excited and ground state populations using chirped pulses.[14] Stimulated emission competes with fluorescence as laser intensity increases, but peak intensity is not the only factor for enhancing stimulated emission. Negatively chirped pulses, for example, deplete excited state population by stimulated emission.[9,14−16] Bardeen et al. carried out a study on coherent control of electronic population.[17] The optimization algorithm found maximum excited state population for positively chirped pulses, consistent with Bardeen's previous results.[11] Unfortunately, their algorithm explored only a small subset of possible phases. Therefore, it is unclear what is required to enhance stimulated emission from molecules in solution because of inter- and intramolecular energy relaxation, solvation dynamics, and electronic dephasing occurring on femtosecond to picosecond time scales. Maximum stimulated emission, therefore, should depend on time, frequency, and phase characteristics of the pulse. For example, fluorescence and stimulated emission have been found to be out-of-phase from each other.[18] More recent experiments on the effect of pulse shaping on stimulated emission following a white-light probe pulse found 1.4× enhancement.[19] The use of separate pump and probe pulses in that work prevented the determination of phase dependence between excitation and stimulated emission.

Here we explore stimulated emission resulting from the third-order polarization of cyanine dye molecules in solution when using a spectral phase step function. Two-photon

Received: February 26, 2016
Revised: March 9, 2016
Published: March 9, 2016

DOI: 10.1021/acs.jpca.6b02010
J. Phys. Chem. A 2016, 120, 2002−2008

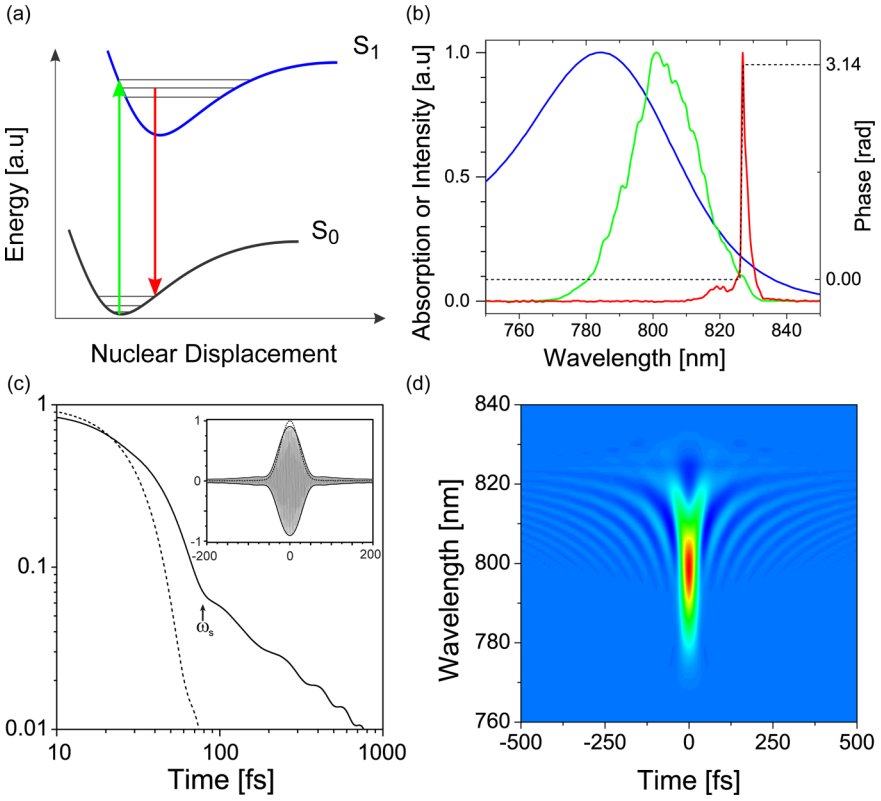

Figure 1. (a) Jablonski diagram showing the excitation pulse (green) and stimulated emission (red) between the ground and excited states. (b) Normalized absorption spectrum of IR125 in methanol (blue), laser excitation spectrum (green), and unfiltered stimulated emission spectrum (red) due to a π-phase step (dashed black) on the excitation spectrum. (c) Double-logarithmic plot of the electric field amplitude of a TL pulse (dashed) and a pulse having a π-phase step at 826.5 nm on the excitation spectrum (black). Inset shows the real part of the electric field (gray) and electric field amplitude (black) for the phase-modulated pulse along with the electric field amplitude of the TL pulse (dashed). (d) Corresponding Wigner representation of the phase step shaped pulse.

transition control has been particularly successful when using a phase step because of constructive interference occurring at twice the frequency corresponding to the position of the phase step; this control has been reported for atoms as well as large organic molecules.[20−33] The similarity between two-photon excitation and coherent anti-Stokes Raman scattering (CARS) led to a phase step being used to enhance CARS signals.[34,35] Under direct resonance with a transition, a phase step has been used on isolated atoms and diatomics, detecting the resonant features as the phase step is scanned within the bandwidth of the excitation pulse.[27,36−38] There is only one case when the transmitted laser and resulting third-order polarization has been analyzed theoretically when using a phase step,[39] and that study was inspired by the results being presented here.

We chose Indocyanine Green, also known as IR125, or Cardiogreen for our experiments, the same molecule used by Bardeen et al.[17] IR125 contains two 1,1-dimethylbenzo[*e*]-indole moieties connected by a seven-carbon conjugated polyene chain and has been studied extensively because of its low toxicity and fast elimination, making it ideal for *in vivo* fluorescent imaging and photodynamic therapy.[40,41] Cyanine dyes in general are also good models for understanding rhodopsin photoisomerization.[42] Indocyanine Green has an absorption maximum in methanol at 784 nm, fluorescence maximum at 837 nm, quantum yield of 0.132, and coherence dephasing time of ∼100 fs.[43,44]

The purpose of this study is to determine the optimum characteristics of a femtosecond pulse for enhancing stimulated emission and concomitantly excited state depletion beyond what can be achieved through properly timed pump−probe pulses or chirped pulses. Here we refer to the third-order polarization resulting from the interaction with a single phase-shaped pulse and not to the stimulated emission often associated with laser amplification where a pump laser creates population inversion and a seed pulse with very different characteristics is amplified through stimulated emission.[19] We chose phase step functions because the corresponding time-domain ultrafast pulses are compact and have a temporally long out-of-phase component. Using $\pm\pi/2$-step phase functions, we explore if phase is of importance beyond the presence of a sharp step. Finally, we compare results from a number of measurements including linear chirp, cubic phase, and pump−probe type excitation.

EXPERIMENTAL METHODS

A Ti:sapphire regenerative amplifier (∼800 μJ, 1 kHz) centered at 800 nm and a diffractive LCOS based 4-*f* pulse shaper (MIIPS-HD, Biophotonic Solutions Inc.) were used to prepare the shaped ultrafast pulses. The pulse shaper was used to measure and correct high-order phase distortions from the amplified laser output and produce transform-limited pulses at the sample using MIIPS.[45] The shaper was then used to introduce the desired phase functions; typically, the shorter wavelengths had a constant zero phase and the longer wavelengths had a constant π-phase.

The laser beam was attenuated and spatially apertured using an iris having a diameter $(1/e^2)$ of ∼4 mm to have uniform

DOI: 10.1021/acs.jpca.6b02010
J. Phys. Chem. A 2016, 120, 2002−2008

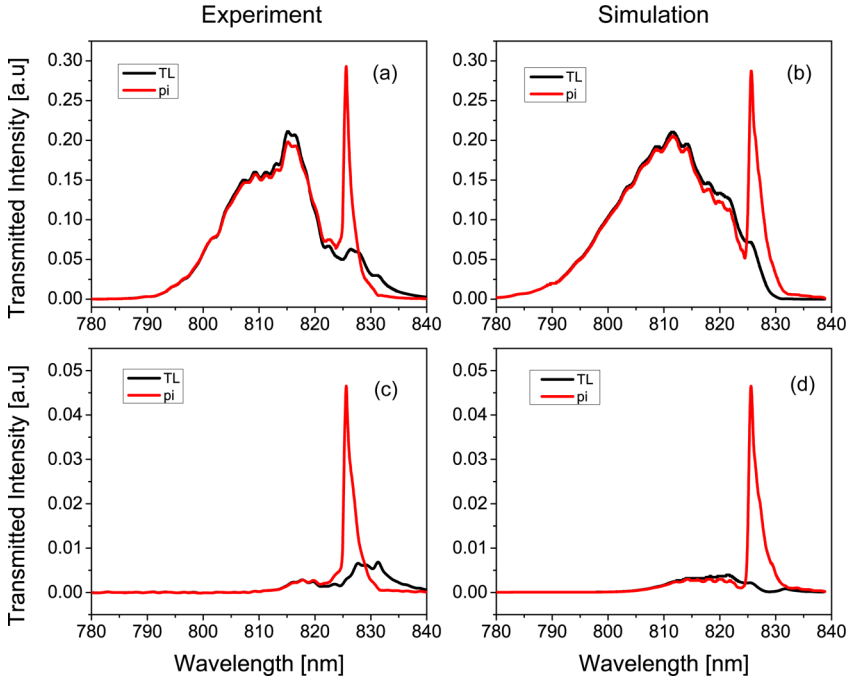

Figure 2. Transmitted signals showing a sharp stimulated emission near 827 nm. Results are shown for TL (black) and shaped pulses having π-phase step at 825.6 nm (red). Experimental results are shown in panels (a) and (c) for samples having an OD ~ 0.7 and 2.5, respectively. Corresponding numerical simulations are shown in panels (b) and (d).

intensity across the beam. Note the beam was not focused. Pulse energy of 40 μJ was used to excite the sample, which corresponds to a peak intensity of ~4 × 10^9 W/cm^2 for the unmodulated transform limited (TL) pulses. Experiments were performed on samples of IR125 in methanol having optical densities of 0.7 and 2.5 in a 1 mm cuvette at room temperature. The calculated probability of excitation ($P = F\sigma$) from first-order perturbation theory using the absorption cross section (σ) of 5.35 × 10^{20} m^2 and photon flux through the sample (F) as 1.39 × 10^{19} m^{-2} was P = 0.7. A schematic diagram of the experiment is shown in Figure 1a. Figure 1b shows the normalized molecular absorption spectrum (blue), spectrum of the laser (green) with spectral phase (dashed black line), and the resulting stimulated emission spectrum (red). The transmitted laser light along with the stimulated emission from the sample was detected ~20 cm away from the cell in the direction of propagation of the beam to minimize fluorescence detection, using a high-resolution compact spectrometer (HR-4000, Ocean Optics). The optical (time and frequency) characteristics of the phase-shaped pulses are shown in Figure 1c,d. The phase-modulated pulse has tails in time domain as compared to a TL pulse, and these long tails decay slowly as can be seen in the double-logarithmic plot in Figure 1c. The temporal profiles of the electric field amplitude for TL (dashed lines) and phase-modulated pulses (solid lines) are shown in the inset along with the real part of the electric field for the phase-modulated pulse. Most importantly, these tails have a corresponding instant optical frequency (ω_s) equal to the frequency of the position of the phase step. A Wigner plot of the pulse with a phase step, shown in Figure 1d, illustrates the discontinuity and the appearance of the long tails.

RESULTS AND DISCUSSION

The spectrum of the transmitted laser light with the prominent stimulated emission peak, along with numerical simulations, are shown in Figure 2 for both transform limited (TL) (black) and π-phase step shaped pulses at 826.5 nm (red). Figures 2a and 2b show experimental and simulated spectra for optical density of OD ~ 0.7, while Figures 2c and 2d show data for OD ~ 2.5. The optically dense medium absorbs most of the laser light, making the stimulated emission more prominent wavelength region. Stimulated emission generated by TL pulses is observed near 827 nm in Figures 2a and 2c. The sharp narrow-band emission near 827 nm is observed when using π-phase step shaped pulses. Stimulated emission enhancement factors (shaped/TL) at 827 nm for phase step shaped pulses of 6× and 14× were observed for 0.7 and 2.5 OD solutions. The enhanced feature was found to grow exponentially with laser intensity (see Supporting Information and Figure S1).

The phase and sign of the phase dependence on the observed stimulated emission enhancement was tested. For π-phase step shaped pulses, no sign dependence is expected; however, when using $+\pi/2$ and $-\pi/2$ phase step shaped pulses sign dependence in the observed enhancement was observed as shown in Figure 3.

Conceptually we understand the observed enhancement of the coherent processes as follows. The phase step modulated pulse has two components in the time domain: a strong short pulse and a much weaker long pulse as shown in Figure 1c. The bulk of the strong pulse excites the system and the tail of the phase-modulated pulse having the step frequency imprinted on it interacts with the molecules in the excited state after a given time and coherently induces stimulated emission. For higher OD samples, the tail of the pulse encounters a population inversion at the longer wavelengths, which leads to further amplification. Both timing and phase of the excitation pulse are essential to observe the enhancement as evidenced by results from $+\pi/2$ and $-\pi/2$ phase steps at 820.3 nm in Figure 3. While the $+\pi/2$ phase step leads to enhancement in the signal

DOI: 10.1021/acs.jpca.6b02010
J. Phys. Chem. A 2016, 120, 2002−2008

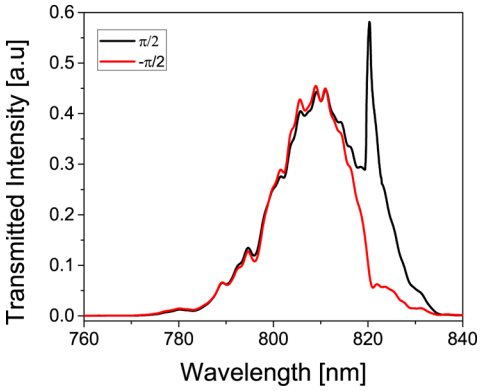

Figure 3. Experimental stimulated emission spectra when excited with laser pulses having a $+\pi/2$ (black) and $-\pi/2$ (red) phase step modulation at 820.3 nm from a sample of IR 125 in methanol having OD = 0.4.

near the step position, the $-\pi/2$ step leads to a depletion in the stimulated emission spectrum near the step position.

The hypothesis that the out-of-phase tail of the π-phase step shaped pulse leads to the enhanced stimulated emission was tested by three different pulse-shaping strategies; results are shown in Figure 4. First, delaying the spectral components with wavelengths longer than 815 nm with respect to the rest of the excitation spectrum resulted in a significant increase in stimulated emission when the probe arrives after the pump pulse, with a maximum observed at 94 fs delay (see Figure 4a). The maximum signal corresponds to the point when the linear phase used to delay the pulse has a π-phase shift at 826 nm with respect to the pump pulse as shown in Figure 4a, inset. The measured spectra corresponding to the minimum (black, at delay of −320 fs) and maximum enhancement (red, at delay of 94 fs) are shown in Figure 4b. Second, a positive cubic spectral phase creates a pulse with a fast rise and a slow decay; the time ordering is reversed for negative cubic functions. The enhancement observed, shown in Figure 4c, was very similar

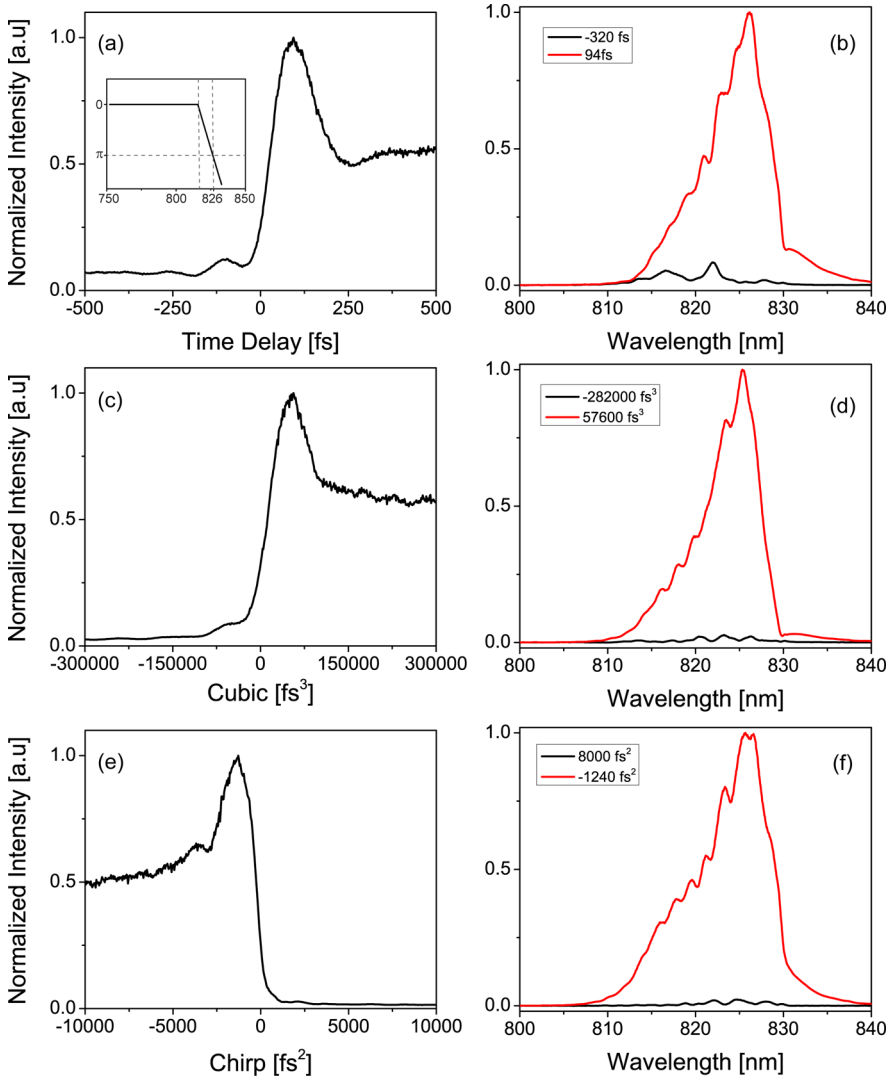

Figure 4. Experimentally measured enhanced transmissions as a function of phase shaping. (a) Integrated transmission measured as a function of time delay of the spectral components with wavelengths longer than 815 nm with respect to the rest of the pulse; (b) corresponding spectra for maximum (red) and minimum (black) delay values. (c) Integrated transmission measured as a function of a cubic phase; (d) corresponding spectra for maximum (red) minimum (black) cubic phase values. (e) Integrated transmission measured as a function of linear chirp; (f) corresponding spectra for the maximum (red) and minimum (black) chirp values.

DOI: 10.1021/acs.jpca.6b02010
J. Phys. Chem. A 2016, 120, 2002−2008

to the pump−probe results. No enhancement was observed for negative cubic phases when the tail arrives before the main pulse. The spectra corresponding to the minimum (black, for cubic phase of −282 000 fs^3) and maximum (red, for cubic phase of 56 700 fs^3) are shown in Figure 4d. Third, negatively chirped pulses, having higher frequencies arriving before the lower frequencies, were also found to enhance stimulated emission as shown in Figure 4e. Spectra observed for minimum (black, for 8000 fs^2) and maximum (red, −1240 fs^2) enhancements are shown in Figure 4f.

The relative enhancement compared to TL pulses measured for different phases has been quantified by either comparing the intensity of the wavelength component corresponding to the maximum (first column) or by comparing the integrated area under the spectrum (second column), as listed in Table 1. The

Table 1. Stimulated Emission Enhancement Comparison between Shaped and TL Pulses

phase type	$I^{shaped}(\lambda_{max})/I^{TL}(\lambda_{max})$	I^{shaped}/I^{TL}
π-step	14	8.4
pump−probe	6.2	8.6
cubic	13	9
chirp	9	8.4

stimulated emission enhancement was found highest for π-step shaped pulses, followed closely by cubic phase shaped pulses. When the enhancement was measured as the area under the spectrum, then all pulse shapes lead to similar enhancement. The enhancement produced by π-shaped pulses is spectrally narrower than for the other pulse shapes.

Theoretical Model and Numerical Calculations. The experimentally measured signal is a coherent sum of the laser field and the fields generated due to the polarization of the sample $E_{signal}(t) = E_{exitation}(t) + E_{sample}(t)$. The fields are proportional to the phase shifted laser-induced polarization $E_{sample}(t) = iP(t)$, which is the sum of linear and nonlinear polarizations, proportional to the microscopic electronic coherences of the dye molecules in solution $P(t) \propto \rho(t)$. The electronic coherence of the molecule ρ_{eg} is defined as the sum of the nondiagonal elements of the density matrix between the ground and excited states. We used time-domain perturbation theory to calculate the first-order $\rho_{eg}^{(1)}$ and third-order $\rho_{eg}^{(3)}$ density-matrix elements of the system. The total electric field emitted by the sample was calculated as $E_{signal}(t) = E_{exitation}(t) + i\alpha[\rho_{eg}^{(1)}(t) + \rho_{eg}^{(3)}(t)]$, where α is a parameter describing the relative contribution between the laser field and the field generated by the sample. Attenuation of the laser by the optically dense sample was described by first-order perturbation theory, and the constant α was adjusted accordingly to fit the experimental data. The simulated signal was multiplied by the fluorescence spectrum for the dye in order to account for the cooperative amplification observed for high OD solutions.

A schematic representation of the energy levels and states used in our theory and numerical simulations is given in Figure 5. The excited electronic state was approximated by a collection of vibronic states with excitation cross section proportional to the experimental absorption spectrum, and the dephasing rate for the individual levels (γ) had a value of 10^{13} fs^{-1}. The excitation cross section takes into account displacement in coordinate space between ground and excited states. We have found that using third-order perturbation theory gives adequate description of the experimental results, and we did confirm it

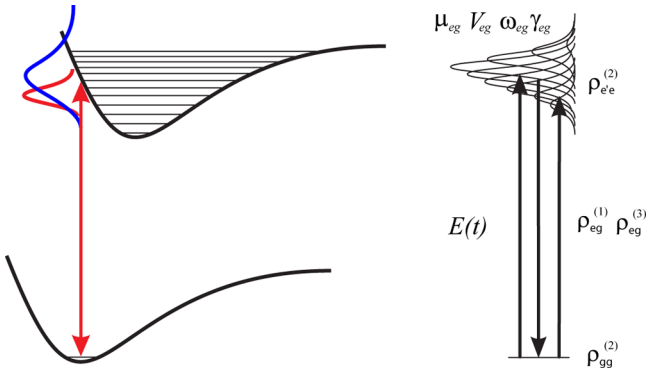

Figure 5. Schematic diagram of the potential energy curves for the ground and excited states of IR125. (left) Note the schematic representation of the excited state and its broad and smooth absorption spectrum (blue) and the laser spectrum (red). The double-headed arrow indicates the presence of nonlinear optical transitions within the bandwidth of the laser. (right) Reduced representation of the system used for the density matrix calculations used here. Notice how the collection of homogeneously broadened excited states mimic the broad absorption spectrum.

using fifth-order perturbation theory and comparing with the nonperturbative solution of the quantum Liouville equation of motion.

The nonlinear component $\rho_{eg}^{(3)}(t)$ is responsible for the measured stimulated emission; therefore, time domain third-order perturbation theory closely approximates the results obtained as shown in Figures 1b,d. The measured spectrum was compared to the Fourier transform of the calculated total field in the time domain $S(\omega) = |\int E_{signal}(t)e^{i\omega t}\, dt|^2$. Absorption of the laser pulse resulting from propagation in dense media and its influence on the measured stimulated emission were calculated by considering thin sample layers, where absorption within each layer is small enough that perturbation theory applies. The output field from one layer was used as input field for the subsequent thin layer. To accurately simulate results for OD = 0.7 and 2.5 we used 3 and 6 thin slices, respectively, and reproduced the exponential attenuation predicted by Beer−Lambert's law. Results from our simulations, shown in Figure 2, successfully reproduce the observed enhancements in stimulated emission. Given that our results, which do not take into account energy relaxation, successfully reproduce the observed signals, we conclude that the stimulated emission observed takes place within the pulse duration. This finding is reinforced by the fact that nonlinear optical interaction must occur while the system is still within the Franck−Condon spectral window accessible by the laser. We carried out upconversion measurement on the stimulated emission and found it to be short-lived (<100 fs). Additional details about the density matrix calculations are provided in the Supporting Information.

CONCLUSIONS

Shaped femtosecond pulses are found to enhance stimulated emission significantly. For moderate concentrations (OD ∼ 0.7), attenuation of the blue part of the excitation spectrum is observed, and a sharp spectral phase step on the red side of the spectrum leads to a narrow factor of 6 enhancement of the emitted spectrum at the step position. For optically dense samples (OD ∼ 2.5) enhancements greater than an order of magnitude are observed through amplification of the electric field generated from the third-order polarization (see

DOI: 10.1021/acs.jpca.6b02010
J. Phys. Chem. A 2016, 120, 2002−2008

Supporting Information). The experimental signals are simulated using third-order perturbation theory. Based on theory, numerical simulations, and a number of control experiments, we are able to provide a conceptual framework for our observations. We attribute the enhancement to the temporal profile of the excitation pulse causing fast population transfer to the excited state followed by a weak tail responsible for interacting with the excited state population and enhancing stimulated emission. Our findings show that a simple phase step can cause order-of-magnitude stimulated emission enhancements.

Our findings are important from a fundamental point of view and may find practical application in the transmission of signals through absorbing media or in some form of microscopy. We have previously found that enhanced stimulated emission leads to a reduction in spontaneous fluorescence.[14] Within the context of pulse shaping, the π-phase step is one of the most used and best understood functions especially when involving multiphoton excitation.[45−48] Our measurements illustrate and explain the outcome of the interaction of shaped pulses with molecules resonant with the excitation pulse. Finally, in the context of Indocyanine Green being the only FDA approved infrared dye and an important photodynamic therapy drug, our findings may point to strategies for enhancing fluorescence or production of singlet oxygen for tumor destruction, given the ability of shaped pulses to control excited state population.

■ ASSOCIATED CONTENT

Supporting Information

The Supporting Information is available free of charge on the ACS Publications website at DOI: 10.1021/acs.jpca.6b02010.

Laser power dependence of the enhanced emission and details on the density matrix calculations (PDF)

■ AUTHOR INFORMATION

Corresponding Author

*E-mail dantus@msu.edu; Tel +1 (517) 355-9715 x314 (M.D.).

Notes

The authors declare no competing financial interest.

■ ACKNOWLEDGMENTS

This material is based upon work supported by the National Science Foundation under Grant NSF CHE-1464807; this support is gratefully acknowledged. Discussions with Profs. Shaul Mukamel and Warren Beck are also sincerely acknowledged.

■ REFERENCES

(1) Mukamel, S. *Principles of Nonlinear Optical Spectroscopy*; Oxford University Press: New York, 1995; p xviii, 543 pp.

(2) Cho, M.; Scherer, N. F.; Fleming, G. R.; Mukamel, S. Photon Echoes and Related Four-Wave-Mixing Spectroscopies Using Phase-Locked Pulses. *J. Chem. Phys.* **1992**, *96*, 5618−5629.

(3) Joo, T.; Jia, Y.; Yu, J. Y.; Lang, M. J.; Fleming, G. R. Third-Order Nonlinear Time Domain Probes of Solvation Dynamics. *J. Chem. Phys.* **1996**, *104*, 6089−6108.

(4) Fleming, G. R.; Cho, M. Chromophore-Solvent Dynamics. *Annu. Rev. Phys. Chem.* **1996**, *47*, 109−134.

(5) Hamm, P.; Lim, M.; Hochstrasser, R. M. Structure of the Amide I Band of Peptides Measured by Femtosecond Nonlinear-Infrared Spectroscopy. *J. Phys. Chem. B* **1998**, *102*, 6123−6138.

(6) Brixner, T.; Mancal, T.; Stiopkin, I. V.; Fleming, G. R. Phase-Stabilized Two-Dimensional Electronic Spectroscopy. *J. Chem. Phys.* **2004**, *121*, 4221−4236.

(7) Jonas, D. M. Two-Dimensional Femtosecond Spectroscopy. *Annu. Rev. Phys. Chem.* **2003**, *54*, 425−463.

(8) Bremer, M. T.; Wrzesinski, P. J.; Butcher, N.; Lozovoy, V. V.; Dantus, M. Highly Selective Standoff Detection and Imaging of Trace Chemicals in a Complex Background Using Single-Beam Coherent Anti-Stokes Raman Scattering. *Appl. Phys. Lett.* **2011**, *99*, 101109-1−101109-3.

(9) Konar, A.; Lozovoy, V. V.; Dantus, M. Solvent Environment Revealed by Positively Chirped Pulses. *J. Phys. Chem. Lett.* **2014**, *5*, 924−928.

(10) Nairat, M.; Konar, A.; Kaniecki, M.; Lozovoy, V. V.; Dantus, M. Investigating the Role of Human Serum Albumin Protein Pocket on the Excited State Dynamics of Indocyanine Green Using Shaped Femtosecond Laser Pulses. *Phys. Chem. Chem. Phys.* **2015**, *17*, 5872−5877.

(11) Cerullo, G.; Bardeen, C. J.; Wang, Q.; Shank, C. V. High-Power Femtosecond Chirped Pulse Excitation of Molecules in Solution. *Chem. Phys. Lett.* **1996**, *262*, 362−368.

(12) Nibbering, E. T. J.; Wiersma, D. A.; Duppen, K. Ultrafast Nonlinear Spectroscopy with Chirped Optical Pulses. *Phys. Rev. Lett.* **1992**, *68*, 514−517.

(13) Duppen, K.; de Haan, F.; Nibbering, E. T. J.; Wiersma, D. A. Chirped Four-Wave Mixing. *Phys. Rev. A: At., Mol., Opt. Phys.* **1993**, *47*, 5120−5137.

(14) Konar, A.; Lozovoy, V. V.; Dantus, M. Solvation Stokes-Shift Dynamics Studied by Chirped Femtosecond Laser Pulses. *J. Phys. Chem. Lett.* **2012**, *3*, 2458−2464.

(15) Cao, J. S.; Bardeen, C. J.; Wilson, K. R. Molecular "Pi Pulse" for Total Inversion of Electronic State Population. *Phys. Rev. Lett.* **1998**, *80*, 1406−1409.

(16) Bardeen, C. J.; Yakovlev, V. V.; Squier, J. A.; Wilson, K. R. Quantum Control of Population Transfer in Green Fluorescent Protein by Using Chirped Femtosecond Pulses. *J. Am. Chem. Soc.* **1998**, *120*, 13023−13027.

(17) Bardeen, C. J.; Yakovlev, V. V.; Wilson, K. R.; Carpenter, S. D.; Weber, P. M.; Warren, W. S. Feedback Quantum Control of Molecular Electronic Population Transfer. *Chem. Phys. Lett.* **1997**, *280*, 151−158.

(18) Konar, A.; Shah, J. D.; Lozovoy, V. V.; Dantus, M. Optical Response of Fluorescent Molecules Studied by Synthetic Femtosecond Laser Pulses. *J. Phys. Chem. Lett.* **2012**, *3*, 1329−1335.

(19) van der Walle, P.; Milder, M. T. W.; Kuipers, L.; Herek, J. L. Quantum Control Experiment Reveals Solvation-Induced Decoherence. *Proc. Natl. Acad. Sci. U. S. A.* **2009**, *106*, 7714−7717.

(20) Meshulach, D.; Silberberg, Y. Coherent Quantum Control of Multiphoton Transitions by Shaped Ultrashort Optical Pulses. *Phys. Rev. A: At., Mol., Opt. Phys.* **1999**, *60*, 1287−1292.

(21) Dudovich, N.; Dayan, B.; Gallagher Faeder, S. M.; Silberberg, Y. Transform-Limited Pulses Are Not Optimal for Resonant Multiphoton Transitions. *Phys. Rev. Lett.* **2001**, *86*, 47−50.

(22) Dudovich, N.; Oron, D.; Silberberg, Y. Coherent Transient Enhancement of Optically Induced Resonant Transitions. *Phys. Rev. Lett.* **2002**, *88*, 123004-1−123004-4.

(23) Gandman, A.; Chuntonov, L.; Rybak, L.; Amitay, Z. Coherent Phase Control of Resonance-Mediated (2 + 1) Three-Photon Absorption. *Phys. Rev. A: At., Mol., Opt. Phys.* **2007**, *75*, 031401-1−031401-4.

(24) Gandman, A.; Chuntonov, L.; Rybak, L.; Amitay, Z. Pulse-Bandwidth Dependence of Coherent Phase Control of Resonance-Mediated Three-Photon Absorption. *Phys. Rev. A: At., Mol., Opt. Phys.* **2007**, *76*, 053419-1−053419-9.

(25) Chuntonov, L.; Rybak, L.; Gandman, A.; Amitay, Z. Enhancement of Intermediate-Field Two-Photon Absorption by Rationally Shaped Femtosecond Pulses. *Phys. Rev. A: At., Mol., Opt. Phys.* **2008**, *77*, 021403-1−021403-4.

DOI: 10.1021/acs.jpca.6b02010
J. Phys. Chem. A 2016, 120, 2002−2008

(26) Amitay, Z.; Gandman, A.; Chuntonov, L.; Rybak, L. Multichannel Selective Femtosecond Coherent Control Based on Symmetry Properties. *Phys. Rev. Lett.* **2008**, *100*, 193002-1−193002-4.
(27) Form, N. T.; Whitaker, B. J.; Meier, C. Enhancing the Probability of Three-Photon Absorption in Iodine through Pulse Shaping. *J. Phys. B: At., Mol. Opt. Phys.* **2008**, *41*, 074011-1−074011-9.
(28) Zhang, S.; Zhang, H.; Jia, T. Q.; Wang, Z. G.; Sun, Z. R. Coherent Control of Two-Photon Transitions in a Two-Level System with Broadband Absorption. *Phys. Rev. A: At., Mol., Opt. Phys.* **2009**, *80*, 043402-1−043402-4.
(29) Zhang, S.; Lu, C.; Jia, T.; Qiu, J.; Sun, Z. Control of Resonance Enhanced Multi-Photon Ionization Photoelectron Spectroscopy by Phase-Shaped Femtosecond Laser Pulse. *J. Chem. Phys.* **2012**, *137*, 174301-1−174301-5.
(30) Zhang, S.; Lu, C.; Jia, T.; Qiu, J.; Sun, Z. Quantum Control of Femtosecond Resonance-Enhanced Multiphoton-Ionization Photoelectron Spectroscopy. *Phys. Rev. A: At., Mol., Opt. Phys.* **2013**, *88*, 043437-1−043437-5.
(31) Zhang, S.; Zhu, J.; Lu, C.; Jia, T.; Qiu, J.; Sun, Z. High-Resolution Resonance-Enhanced Multiphoton-Ionization Photoelectron Spectroscopy of Rydberg States via Spectral Phase Step Shaping. *RSC Adv.* **2013**, *3*, 12185−12189.
(32) Xu, S.; Ding, J.; Lu, C.; Jia, T.; Zhang, S.; Sun, Z. Effect of Laser Spectral Bandwidth on Coherent Control of Resonance-Enhanced Multiphoton-Ionization Photoelectron Spectroscopy. *J. Chem. Phys.* **2014**, *140*, 084312-1−084312-5.
(33) Gandman, A.; Rybak, L.; Amitay, Z. Observation and Symmetry-Based Coherent Control of Transient Two-Photon Absorption: The Bright Side of Dark Pulses. *Phys. Rev. Lett.* **2014**, *113*, 043003-1−043003-5.
(34) Oron, D.; Dudovich, N.; Yelin, D.; Silberberg, Y. Narrow-Band Coherent Anti-Stokes Raman Signals from Broad-Band Pulses. *Phys. Rev. Lett.* **2002**, *88*, 063004-1−0630004-4.
(35) Postma, S.; van Rhijn, A. C. W.; Korterik, J. P.; Gross, P.; Herek, J. L.; Offerhaus, H. L. Application of Spectral Phase Shaping to High Resolution Cars Spectroscopy. *Opt. Express* **2008**, *16*, 7985−7996.
(36) Bayer, T.; Wollenhaupt, M.; Sarpe-Tudoran, C.; Baumert, T. Robust Photon Locking. *Phys. Rev. Lett.* **2009**, *102*, 023004-1−023004-4.
(37) Wollenhaupt, M.; Bayer, T.; Vitanov, N. V.; Baumert, T. Three-State Selective Population of Dressed States Via Generalized Spectral Phase-Step Modulation. *Phys. Rev. A: At., Mol., Opt. Phys.* **2010**, *81*, 053422-1−053422-9.
(38) Bruner, B. D.; Suchowski, H.; Vitanov, N. V.; Silberberg, Y. Strong-Field Spatiotemporal Ultrafast Coherent Control in Three-Level Atoms. *Phys. Rev. A: At., Mol., Opt. Phys.* **2010**, *81*, 063410-1−063410-5.
(39) Glenn, R.; Mukamel, S. Multidimensional Spectroscopy with a Single Broadband Phase-Shaped Laser Puls. *J. Chem. Phys.* **2014**, *140*, 144105-1−144105-13.
(40) Schaafsma, B. E.; Mieog, J. S. D.; Hutteman, M.; van der Vorst, J. R.; Kuppen, P. J. K.; Löwik, C. W. G. M.; Frangioni, J. V.; van de Velde, C. J. H.; Vahrmeijer, A. L. The Clinical Use of Indocyanine Green as a near-Infrared Fluorescent Contrast Agent for Image-Guided Oncologic Surgery. *J. Surg. Oncol.* **2011**, *104*, 323−332.
(41) Yannuzzi, L. A.; Slakter, J. S.; Gross, N. E.; Spaide, R. F.; Costa, D. L. L.; Huang, S. J.; Klancnik, J. M. J.; Aizman, A. Indocyanine Green Angiography-Guided Photodynamic Therapy for Treatment of Chronic Central Serous Chorioretinopathy: A Pilot Study. *Retina* **2003**, *23*, 288−298.
(42) Wald, G. The Molecular Basis of Visual Excitation. *Nature* **1968**, *219*, 800−807.
(43) Park, S.; Park, J.-S.; Joo, T. Solvation Dynamics by Coherence Period Resolved Transient Grating. *J. Phys. Chem. A* **2011**, *115*, 3973−3979.
(44) Konar, A.; Lozovoy, V. V.; Dantus, M. Electronic Dephasing of Molecules in Solution Measured by Nonlinear Spectral Interferometry. *Sci. Lett.* **2015**, *4*, 141.
(45) Coello, Y.; Lozovoy, V. V.; Gunaratne, T. C.; Xu, B. W.; Borukhovich, I.; Tseng, C. H.; Weinacht, T.; Dantus, M. Interference without an Interferometer: A Different Approach to Measuring, Compressing, and Shaping Ultrashort Laser Pulses. *J. Opt. Soc. Am. B* **2008**, *25*, A140−A150.
(46) Brixner, T.; Damrauer, N. H.; Niklaus, P.; Gerber, G. Photoselective Adaptive Femtosecond Quantum Control in the Liquid Phase. *Nature* **2001**, *414*, 57−60.
(47) Walowicz, K. A.; Pastirk, I.; Lozovoy, V. V.; Dantus, M. Multiphoton Intrapulse Interference. 1. Control of Multiphoton Processes in Condensed Phases. *J. Phys. Chem. A* **2002**, *106*, 9369−9373.
(48) Lozovoy, V. V.; Pastirk, I.; Walowicz, K. A.; Dantus, M. Multiphoton Intrapulse Interference. Ii. Control of Two- and Three-Photon Laser Induced Fluorescence with Shaped Pulses. *J. Chem. Phys.* **2003**, *118*, 3187−3196.

DOI: 10.1021/acs.jpca.6b02010
J. Phys. Chem. A 2016, 120, 2002−2008